Check for updates

BRIEF COMMUNICATION   **OPEN**

Lightweight and flexible Cu(In,Ga)Se$_2$ solar minimodules: toward 20% photovoltaic efficiency and beyond

Shogo Ishizuka[1] ✉, Yukiko Kamikawa[1] and Jiro Nishinaga[1]

Lightweight and flexible photovoltaic solar cells and modules are promising technologies that may result in the wide usage of light-to-electricity energy conversion devices. This communication presents the prospects of Cu(In,Ga)Se$_2$ (CIGS)-based lightweight and flexible photovoltaic devices. The current status of flexible CIGS minimodules with photovoltaic efficiency values greater than 18% and future directions to enhance their efficiency values toward >20% are discussed. The effects of cell separation edges, which are formed through a mechanical, laser, or photolithography scribing process used to fabricate solar cells and modules, on the device performance are also discussed. We found that mechanically scribed CIGS device edges, which are present in conventional solar cells and modules, cause deterioration of device performance. In other words, further improvement is expected with appropriate passivation/termination treatment of the edges or replacing mechanical scribing with a damage-free separation process.

INTRODUCTION

The development of lightweight and flexible photovoltaic solar cells that can be installed in places with severe weight restrictions, curved surfaces, or places with difficulty in the utilization of conventional silicon (Si)-based solar cells is expected to result in the widespread use of solar energy. Thin-film photovoltaic technologies, including Cu(In,Ga)Se$_2$ (CIGS), CdTe, and other chalcogenide and organic-inorganic hybrid perovskite solar cells, are promising for realizing this type of application, namely, highly efficient, cost-effective, and lightweight flexible photovoltaic devices[1]. Among thin-film photovoltaic technologies, CIGS-based solar cells are an attractive option owing to their advantages of relatively high energy conversion efficiency, long-term stability, relatively short energy payback time, and small carbon footprint of products[2]. To date, the photovoltaic efficiency value of CIGS-based solar modules fabricated using rigid glass substrates has been approaching 20%; for instance, solar modules with photovoltaic efficiency values of 19.8% (Avancis, 665.4 cm^2, 110 cells)[3,4], 19.8% (Solar Frontier, 24.2 cm^2, 12 cells)[5], and 19.2% (Solar Frontier, 841 cm^2, 70 cells)[5] are currently available in the literature.

One of the notable features of CIGS-based modules is that they can be fabricated using grid electrodes and monolithically interconnected structures. The grid electrode structure comprises independent cells connected with metal bus-bar and grid electrodes, similar to the structure of conventional Si-based solar modules, whereas the monolithically interconnected structure is fabricated with patterned cells monolithically interconnected on a single substrate (Fig. 1). The highly efficient CIGS solar modules with photovoltaic efficiency values greater than 19% demonstrated on the aforementioned glass substrates have a monolithically interconnected structure. Although both module structures have merits and demerits, it is not a question of whether they are better or not. Nonetheless, a monolithically interconnected structure has the merit of realizing thinner and lighter solar modules, owing to the absence of metal electrodes on the module surface. To date, photovoltaic efficiency values greater than 18% have been demonstrated for CIGS solar (mini)

modules fabricated on non-glass flexible substrates, regardless of the grid electrode[6] or monolithically interconnected structure[7].

In this communication, recent developments in the photovoltaic performance of lightweight and flexible monolithically interconnected CIGS solar minimodules are presented. The issues regarding the development of CIGS solar cells and modules with higher photovoltaic efficiency values are also discussed.

RESULTS AND DISCUSSION

Lightweight and flexible monolithically interconnected CIGS solar minimodules

To obtain enhanced device performance from CIGS-based solar cells and modules, the control of alkali metal doping is essential. The effects of various alkali metals (Li, Na, K, Rb, and Cs) on CIGS thin-film and device properties have been widely studied[8–15]. The use of heavier elements, such as Rb and Cs, has been reported to be more effective in obtaining higher photovoltaic efficiency values[12,13]. In contrast, the aforementioned CIGS submodule with 19.8%-efficiency (Avancis, 665.4 cm^2, 110 cells) was demonstrated using only a relatively light alkali-metal Na-postdeposition treatment (PDT)[4]. This report[4] suggests that the beneficial effect of alkali metal doping depends not only on the alkali metal species but also on the doping methods and processes, including the quantity and timing of the supply of alkali metals and other experimental conditions.

The photovoltaic properties of CIGS solar minimodules #1 and #2 obtained with different alkali metal PDTs in our laboratory are summarized in Table 1. These photovoltaic parameters were obtained from independently certified measurements, which were performed at the Photovoltaic Calibration, Standards, and Measurement Team of the Renewable Energy Research Center, the National Institute of Advanced Industrial Science and Technology (AIST) and the Japan Electrical Safety and Environment Technology Laboratories (JET), respectively, after heat-light soaking (HLS) treatments. Variations in parameters, such as open-circuit voltage (V_{OC}), short-circuit current (I_{SC}), and fill factor (FF), were assumed to be due to the difference in the elemental

[1]Research Institute for Energy Conservation, National Institute of Advanced Industrial Science and Technology, Tsukuba, Japan. ✉email: shogo-ishizuka@aist.go.jp

composition ratio [Ga]/([Ga] + [In]) (GGI) and CdS buffer thickness of these devices instead of the different alkali metal species used for PDT (minimodule #2 had a lower GGI value and a thicker CdS layer than those in minimodule #1; see the "Methods" section). This result indicates that the current technique can demonstrate CIGS minimodules of ~18.5% efficiency on flexible substrates using a monolithically interconnected structure. Figure 2a shows a photograph of the CIGS solar minimodule #1. In comparison with the weight of conventional photovoltaic solar modules in the range of 10–20 kg m^{-2}, the weight of our CIGS minimodules fabricated using 0.2-mm-thick flexible ceramic sheets as the substrate was equivalent to one-tenth of their weight. The beneficial effect of metastable acceptor activation with HLS or heat-bias soaking (HBS) treatments on CIGS small-area solar cells grown with alkali metal PDT has been reported in the literature[16,17]. It was found that a similar beneficial effect of enhancing photovoltaic efficiency values with HLS treatments can be obtained from the CIGS minimodules, irrespective of the alkali metal species used for PDTs, as shown in Fig. 2b. The enhancement in photovoltaic performance was due to improvements in V_{OC} and FF, and this result was similar to that obtained using small-area cells[16,17].

For further development of CIGS photovoltaic devices, enhancement of the photovoltaic efficiency values of small-area cells, namely, the baseline of device performance, is essential. In addition to alkali-metal doping, silver (Ag)- and sulfur (S)-alloying for the modification and control of the energy band structure in CIGS devices, improvement in the bulk crystal quality, and surface and back interface (buffer/CIGS and CIGS/Mo interfaces) modification are the current topics of interest in the CIGS community[4,13,18–23]. These approaches are expected to lead to further enhancements in lightweight and flexible CIGS minimodule efficiency values from the current 18.5% level demonstrated with quaternary CIGS photoabsorbers in this study to >20%[4,13,18–23].
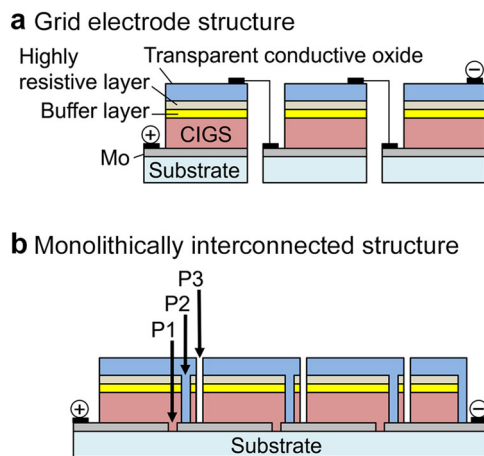

Fig. 1 **Schematic of CIGS solar module structure. a** Grid electrode module. **b** monolithically interconnected module.

Effects of cell separation edges on photovoltaic performance

As mentioned above, the suppression of carrier recombination at the interface and in the bulk of CIGS thin-film devices is important for improving photovoltaic efficiency values. To date, much effort has been devoted to the suppression of recombination at the surface (buffer/CIGS) and back (CIGS/Mo) interfaces and in the bulk of CIGS photoabsorbers, including grain boundaries and grain inside[24]. In addition to these recombination issues, it is suggested that scribed edges of CIGS photoabsorbers, namely, cross-sections (sidewalls) of a CIGS device formed in cell and module fabrication processes, are likely to be one of the important origins resulting in recombination and concomitant degradation of device performance[25]. Nevertheless, to date, there have been only a few discussions on the effect of mechanically scribed edges on photovoltaic performance[25]. Therefore, in this section, the effect of mechanical scribing (MS), which has been used as a standard technique, on photovoltaic performance is comparatively studied with photolithographically formed edges.

MS is usually employed for P2 and P3 patterning processes for monolithically interconnected module fabrication, as shown in Fig. 1b. Laser scribing techniques have been proposed to unify P1–P3 patterning processes[26,27]. Currently, however, a decreasing shunt resistance occurring at laser-scribed edges remains an issue for effective cell separation[27]. A decrease in the resistance is not a problem for P2 edges; however, it leads to significant degradation of the P3 edges owing to the incomplete separation of cell strings. The question now is, whether MS is a perfect separation process, i.e., whether the scribed edges are negligible as recombination
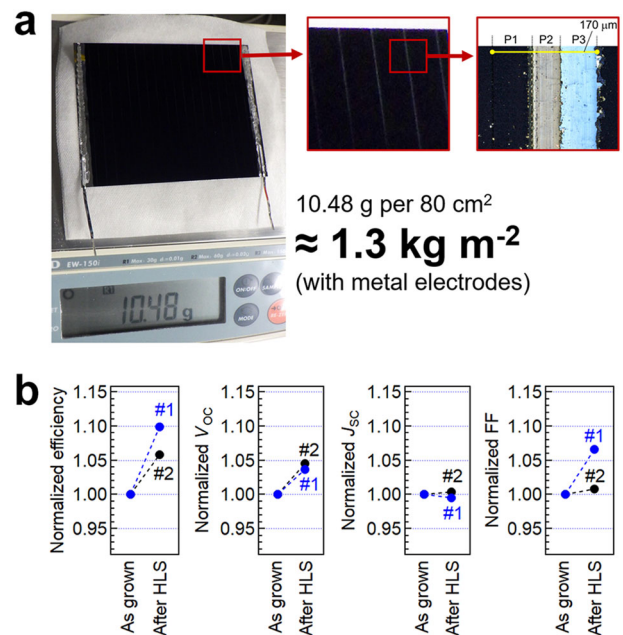

Fig. 2 **CIGS solar minimodule properties. a** Photograph of CIGS solar minimodule #1. **b** Variations in CIGS minimodule properties with HLS treatments. J_{SC}: Short circuit current density.

Table 1.	Performance of lightweight and flexible monolithically interconnected CIGS minimodules.							
Minimodule	PDT	Efficiency (%)	V_{OC} (V)	I_{SC} (mA)	FF (%)	Area (cm^2)	No. of cells	Test center
#1[7]	RbF	18.64	12.70	138.5	72.0	68.0 (d.a.)	17	AIST
#2	NaF + KF	18.5	12.13	136.8	75.8	67.95 (d.a.)	17	JET
d.a. designated area.								

centers and no photovoltaic performance degradation is expected. If not, further improvement can be expected to enhance the photovoltaic performance of CIGS cells and modules with appropriate passivation/termination treatments. Hence, the effect of MS on device performance was studied using small-area (0.5 cm²) cells fabricated on rigid soda-lime glass (SLG) substrates. Notably, only a few institutes, such as the National Renewable Energy Laboratory, have employed a photolithography (PhL) cell separation process until now[28]; thus, there have been a fewer reports regarding the damage effect of conventional MS on photovoltaic performance[25] compared with the use of PhL.

The CIGS small-area cells fabricated using MS and PhL cell separation processes are shown in Fig. 3. Details regarding the CIGS device fabrication pr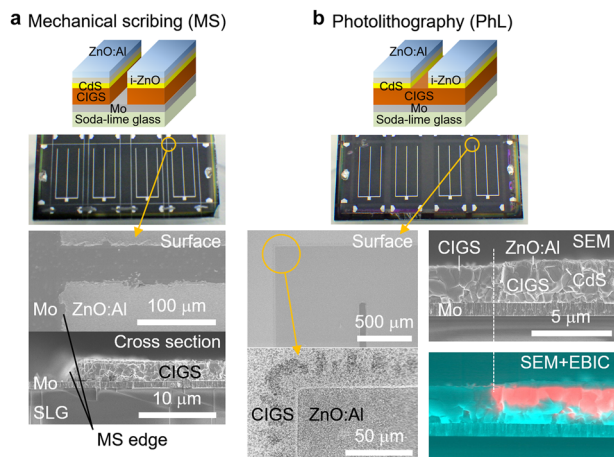ocess can be found in the Methods section. Although PhL may be a relatively expensive and time-consuming process compared with MS, it has been used to precisely define the cell area[28]. As shown in Fig. 3, the cell edge formed with PhL is sharper and thus more precise than that formed with MS. PhL etched only the CdS and upper layers, thus the CIGS layer remained. Nonetheless, electron-beam induced current (EBIC) measurements revealed that the expansion of the space charge region in the CIGS layer was clearly halted on the edge, implying successful cell separation. This is consistent with the constant values observed for J_{SC} and external quantum efficiency (EQE), irrespective of MS or PhL, as shown in Fig. 4.

In this study, variations in the photovoltaic parameters obtained from four types of CIGS cells grown on SLG substrates were examined. These were CIGS solar cells fabricated with (w/) and without (w/o) RbF-PDT using MS or PhL cell separation. No anti-reflection coating (ARC) was used, and no metastable acceptor activation treatment (such as HLS or HBS treatment) was performed before the measurements. Figure 4a shows the data obtained from the eight cells for each type of device. The current density (J)–voltage (V) measurements were performed immediately after the cell separation process. A systematic variation was observed in the photovoltaic efficiency values, and the use of RbF-PDT and PhL led to an enhancement in the performance. It was found that the use of RbF-PDT was effective in enhancing V_{OC} and FF, similar to the results shown in previous reports[12,29], whereas the use of PhL was particularly effective in improving FF (a slight improvement in V_{OC} was also observed). No significant variation was observed in J_{SC}. The J–V and EQE curves obtained from the best cells for each type of device are shown in Fig. 4b, c. The diode parameters obtained from the corresponding cells are summarized in Table 2, where R_{sh}, R_s, A, and J_0 denote the shunt resistance, series resistance, diode ideality factor, and reverse saturation current density, respectively. Variations observed in the J–V and EQE curves were reasonably consistent with the variations in photovoltaic parameters, and the use of RbF-PDT enhanced V_{OC} (Fig. 4b). The use of PhL improved the leakage current, as can be seen in the third quadrant, and no significant variation in EQE was observed regardless of the cell type (Fig. 4c). Notably, the use of
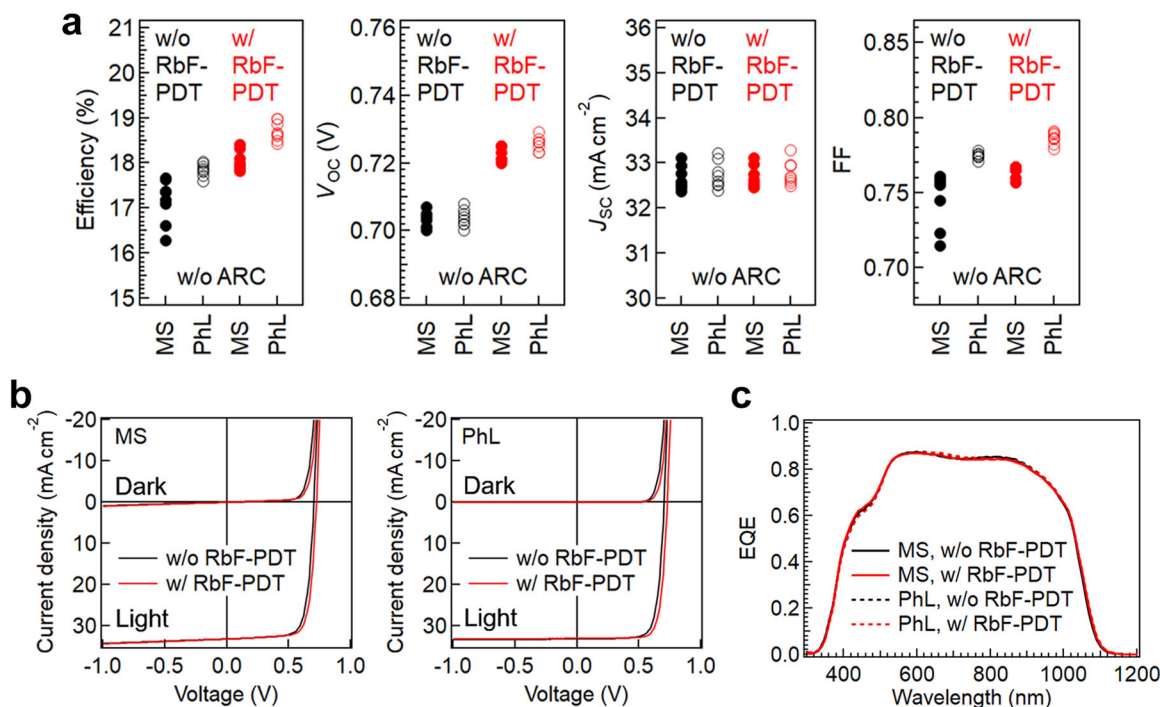

Fig. 3 Scribing edges formed with MS and PhL. a Schematic of MS-separated edges and a corresponding photograph and scanning electron microscopy (SEM) images. **b** Schematic of PhL-separated edges and a corresponding photograph and SEM and EBIC images.

Fig. 4 Comparison of MS- and PhL-separated solar cell properties. a Variations in solar cell parameters. **b** J–V and **c** EQE curves obtained from corresponding cells.

Table 2. Diode parameters obtained for MS- and PhL-separated CIGS solar cells.

Scribing	RbF-PDT	R_{sh} (Ω cm^2)	R_s (Ω cm^2)	A	J_0 (mA cm^{-2})
Dark					
MS	No	1289	0.38	1.46	1.00E-07
MS	Yes	1118	0.46	1.43	4.70E-08
PhL	No	Inf.	0.38	1.40	5.00E-08
PhL	Yes	Inf.	0.25	1.43	3.80E-08
Light					
MS	No	803	0.06	1.71	3.30E-06
MS	Yes	715	0.27	1.54	2.70E-07
PhL	No	5393	0.12	1.66	2.00E-06
PhL	Yes	7102	0.22	1.52	1.90E-07

Inf. Nominally infinite.

PhL led to an increase in R_{sh}, resulting in an improvement in FF, and, thus, photovoltaic efficiency values. The light R_{sh} (R_{sh} obtained under illumination) of typical CIGS cells fabricated with MS was 700–800 Ω cm^2, which was almost consistent with the values obtained in our previous report[30]. In contrast, the light R_{sh} of CIGS cells fabricated with PhL was significantly high and greater than 5000 Ω cm^2, and the dark R_{sh} (R_{sh} obtained under dark conditions) was nominally infinite. The R_{sh} values calculated in this study were lower than those reported in the literature[25,27]. Nonetheless, the MS-separated cells demonstrated relatively high photovoltaic efficiency values of >18%. Of note, these CIGS cells used in this study were fabricated in identical growth batches w/ and w/o RbF-PDT, namely, from the Mo-back contact layer through CIGS photoabsorber layer to ZnO:Al surface electrode layer deposition processes; therefore, only the cell separation process was different. This result indicates that conventional cell edges formed with MS cause a decrease in the R_{sh} values and concomitant degradation of the photovoltaic performance; thus, there is scope for further improvement. The relationship between V_{OC} and J_{SC} is described as

$$V_{OC} = \frac{AkT}{q} ln\left(\frac{J_{SC}}{J_0} + 1\right) \tag{1}$$

where k, T, and q are the Boltzmann constant, temperature, and electron charge, respectively. Equation (1) can be modified in the presence of R_{sh}:

$$V_{OC} = \frac{AkT}{q} ln\left(\frac{J_{ph} - V_{OC}/R_{sh}}{J_0} + 1\right) \tag{2}$$

where J_{ph} is the photocurrent[31]. The effect of R_{sh} is not significant when the J_{ph} is large enough, whereas it becomes important when the J_{ph} is small, namely, under low irradiance conditions[31]. This is experimentally shown in the following subsection.

The A values obtained from MS- and PhL-separated cells showed no significant variation under the dark condition. The variation between MS- and PhL-separated cells under the light condition was almost negligible; however, the cells fabricated with RbF-PDT showed lower A values. This result may indicate the stronger effect of interfacial modification with heavy alkali metal Rb than that of the separation process on parameter A in the presence of photocurrent. A similar variation trend was observed for the J_0 values.

Illumination intensity dependence

One of the important properties required for practical applications of photovoltaic solar cells and modules is their photovoltaic performance under low illumination conditions, irrespective of whether they are used indoor or outdoor. Hence, variations in photovoltaic performance with light intensity (irradiance dependence) were measured under simulated sunlight with neutral density (ND) filters. Figure 5a shows the J–V curves and variations in solar cell parameters measured under various light intensity conditions ranging from 1 to 0.01 sun (nominally equivalent to from 100,000 to 1000 lx). For this experiment, two small-area (0.5 cm^2) single-cells randomly selected from PhL- and MS-separated RbF-PDT CIGS devices with photovoltaic efficiency values of 20.1% and 18.6% at 1 sun (with ARC and without HLS treatments), respectively, were used. It is known that the photovoltaic performance under low illumination conditions significantly depends on R_{sh}, and CIGS cells with relatively low R_{sh} show a steep drop in V_{OC} and FF with decreasing light intensity[31]. This trend could be observed for the MS-separated CIGS cell shown in Fig. 5a. In contrast, the PhL-separated cell showed no such drastic degradation in performance under low illumination conditions. On the contrary, a slight improvement was observed in the photovoltaic efficiency value with decreasing light intensity. Note that the R_{sh} values for the MS and PhL devices calculated at 1 sun were 916 and 4670 Ω cm^2, respectively. These two CIGS cells were fabricated in identical growth batches from the Mo-back contact layer to ZnO:Al surface electrode layer deposition processes; therefore, only the cell separation process was different. The PhL- and MS-separated CIGS cells demonstrated photovoltaic efficiency values ranging from 18.5%–20%; therefore, the difference was not significant at 1 sun, but the difference between the photovoltaic performance, particularly V_{OC} and FF, and concomitant maximum output power (P_{max}) increased with decreasing light intensity. The variation trend observed for the PhL-separated CIGS cell was quite similar to the simulation results of an ideal cell with $R_s \approx 0$ and $R_{sh} \approx$ infinite[31]. As summarized in Table 2, the cell separation processes, MS and PhL, did not affect R_s values but significantly affected R_{sh} values. This result indicates that the effect of the cell separation process on photovoltaic performance, i.e., the MS technique conventionally used for cell and module fabrication, is nonnegligible and an important issue as well as the interface and bulk issues of CIGS devices.

Figure 5b shows the lightweight and flexible CIGS minimodules (size: 8 × 10 cm^2 and 2 × 10 cm^2; P1: laser scribing; P2 and P3: MS, demonstration of products fabricated using a relatively low photovoltaic efficiency [~15% or less] minimodules) generating electricity and lighting a green light-emitting diode under room light (fluorescent tubes) with ~200 lx (nominally equivalent to 0.002 sun) illumination, indicating that CIGS solar modules can be useful light-harvesting devices even under low illumination conditions, such as on the floor in an office. Notably, these CIGS solar minimodules were fabricated using conventional MS for the P3 patterning process, and, thus, further improvements are expected with the modification of the P3 patterning.

The lightweight and flexible CIGS minimodules with photovoltaic efficiency values greater than 18%, shown in the previous section, were also fabricated using MS for P2 and P3 processes. It may be challenging to apply PhL techniques to fabricate large-area modules in practical and industrial production. Nonetheless, the results obtained in this study suggest that the modification of the P3 process, for instance, the use of other patterning processes or effective passivation/termination of the MS edges (this applies to cell edges of grid-electrode structure modules), is a promising approach to further improve CIGS module efficiency values, irrespective of the conventional rigid glass or flexible substrates. The utilization of cost-effective substrate materials, such as insulator-coated steel foils and synthetic resins, is also an
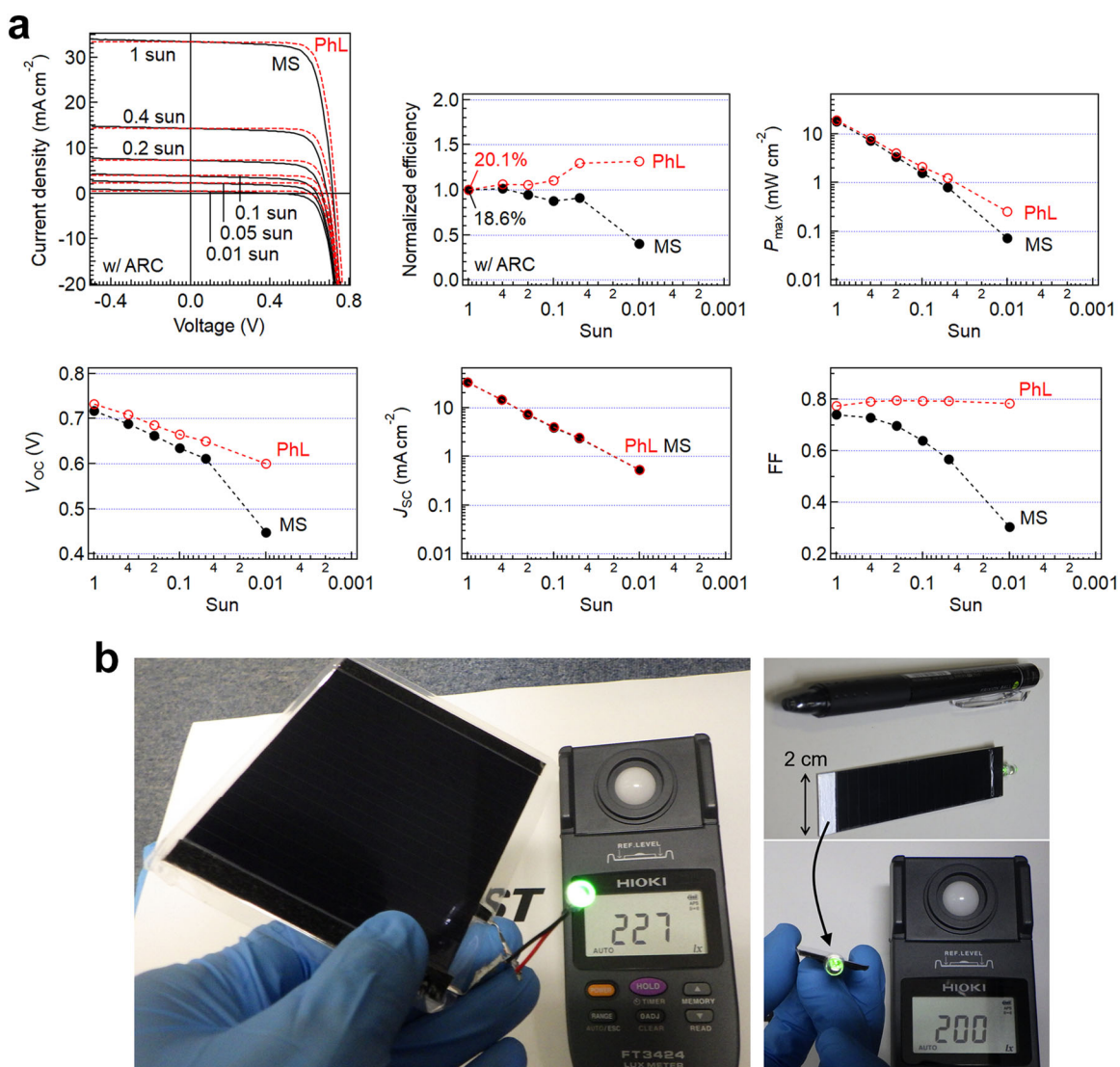
Fig. 5 Light intensity dependence of CIGS solar cells. a *J–V* curves and corresponding solar cell parameter variations observed for 0.5 cm² size PhL-separated (red) and MS-separated (black) CIGS single-cells. **b** Photographs of practical usage of lightweight and flexible CIGS minimodules lighting a green LED under approximately 200 lx illumination.

important factor in the development of flexible photovoltaic solar modules.

In conclusion, we presented the current status and perspective of lightweight and flexible CIGS solar modules. The availability and usefulness of CIGS photovoltaic devices under low illumination conditions have also been suggested. For further development, the improvement of CIGS single-cell performance is essential. Approaches based on material science and device physics, including modification of surface and interface, and bulk crystal quality by alloying with Ag or S, or other elements as well as doping control of alkali metals, are expected to bring further progress in CIGS photovoltaics. In addition, the development of module fabrication processes is expected to result in further enhancements in CIGS photovoltaic performance. It is suggested that mechanically scribed cell edges (equivalent to the side wall of P3 in the module fabrication process) can be an important factor in the degradation of CIGS photovoltaic device performance; therefore, there is room for further improvement in the device fabrication process as well as thin-film bulk material and interfacial properties.

METHODS
Sample preparation
CIGS films (2 μm thick) were grown on Mo (1 μm thick)-coated substrates using a three-stage coevaporation process[32], where (In, Ga)$_2$Se$_3$ precursor films were prepared during the first stage using elemental In, Ga, and Se fluxes evaporated with Knudsen cells at a substrate temperature (T_S) of 350 °C. Elemental Cu and Se fluxes were supplied during the second stage at T_S of 540–550 °C; in the third stage, elemental In, Ga, and Se were supplied using fluxes identical to those employed in the first stage at T_S of 540–550 °C. Sputtered-SLG-coated (75 nm thick) flexible zirconia ceramic sheets[33] and rigid SLG substrates were used for the fabrication of minimodules and small-area cells, respectively. Na- and K-, or Rb-PDT were performed using NaF and KF, or RbF evaporated using Knudsen cells in the CIGS growth chamber. NaF and KF, or RbF were supplied with Se supply following CIGS film growth at T_S of 350 °C for 10 min. The Knudsen cell source temperatures used for NaF, KF, and RbF were 640 °C, 660 °C, and 550 °C, respectively. The CIGS film growth chamber used in this study was designed to deposit uniform films over an area of 100 × 100 mm²; therefore,

nine $30 \times 30\,mm^2$ samples could be grown under nominally identical conditions in a single growth run. The GGI ratio was 0.2–0.3 although the value used for minimodule #1 and small-area cells was slightly higher than that used for minimodule #2. Namely, the GGI and [Cu]/([In]+[Ga]) (CGI) ratios were ~0.25 and 0.9, respectively, for minimodule #1 and small-area cells, and the GGI and CGI ratios were ~0.20 and 0.9, respectively, for minimodule #2, as determined using an electron-probe microanalyzer. After CIGS film growth, a CdS buffer layer was deposited through chemical bath deposition using an aqueous solution comprising $CdSO_4$, NH_2CSNH_2, and ammonia, and water at 80 °C. The thickness of the CdS layer used for minimodule #1 was ~30 nm, whereas the thickness used for minimodule #2 and small-area cells was 50–60 nm. Highly resistive intrinsic ZnO (i-ZnO) and conductive ZnO:Al layers of ~50 and 300 nm, respectively, were deposited via sputtering (sheet resistance: typically 30–40 $\Omega\,cm^2$), and a Ni/Al grid electrode was formed via electron-beam evaporation for solar cell fabrication. For minimodule fabrication, P1 was performed using nanosecond laser scribing (Cyber Laser SPICA532-YVO4; wavelength 532 nm; power 900 mW; frequency 30 kHz; and speed 300 mm s^{-1}) prior to CIGS film growth, whereas the P2 and P3 processes were performed using MS. ZnO layers were deposited using the same sputtering apparatus used for the fabrication of small-area cells; however, the thickness of the ZnO:Al layer was 700 nm for fabricating minimodules (sheet resistance: typically 10 $\Omega\,cm^2$). For fabricating small-area cells, cell separation was performed using MS or PhL for CIGS devices grown in identical growth badges. The PhL process was performed using AZ5200NJ as a photoresist and a pre-baking process at 90 °C for 1 min before light exposure. After PhL developing using a 10-mW lamp for 20 s, the CIGS devices were rinsed with pure water and post-baking was performed at 115 °C for 3 min. Finally, the CdS and ZnO layers on the CIGS surface were removed using HCl solution, followed by rinsing with acetone to remove the photoresist, which was successively rinsed with pure water and dried with N_2 gas blow. In contrast, the MS process was simply performed with a metal cutter. P2 and P3 processes and small-area cell separation were performed using the same MS apparatus.

Measurements of solar minimodule and cell properties
The CIGS minimodule performance was independently measured at AIST and JET. HLS treatments were performed at 95 °C at approximately 1 sun illumination in a N_2-purged box. In-house measurements of small-area cell parameters were performed with a direction from J_{SC} to V_{OC} at 25 °C under 100 mW cm^{-2} (1 sun, AM 1.5 G) illumination and dark conditions. The light intensity was adjusted using ND filters for irradiance dependence measurements. An MgF_2 ARC was used for minimodules #1 and #2 and small-area cells used for irradiance dependence studies (Fig. 5), whereas no ARC was used for RbF-PDT, MS, and PhL comparative studies (Fig. 4). The diode parameters of small-area cells were calculated from light and dark $J–V$ data of the highest photovoltaic efficiency solar cells in each device type (w/ or w/o RbF-PDT and MS or PhL) using the single diode model[34,35]. The R_{sh} values were calculated at voltages ranging from −0.1 to 0.08 V.

SEM and EBIC measurements
SEM and EBIC measurements were performed using a HITACHI S4800 instrument with acceleration voltages of 5 kV and 15 kV for SEM and EBIC measurements, respectively.

DATA AVAILABILITY
The data that support the findings of this study are available from the corresponding author upon reasonable request.

REFERENCES
1. Powalla, M. et al. Thin-film solar cells exceeding 22% solar cell efficiency: an overview on CdTe-, Cu(In,Ga)Se2-, and perovskite-based materials. *Appl. Phys. Rev.* **5**, 041602 (2018).
2. de Wild-Scholten, M. J. (Mariska) Energy payback time and carbon footprint of commercial photovoltaic systems. *Sol. Energy Mater. Sol. Cells* **119**, 296–305 (2013).
3. Green, M. A. et al. Solar cell efficiency tables (Version 60). *Prog. Photovolt. Res. Appl.* **30**, 687–701 (2022).
4. Dalibor, T. CIGSSe module efficiencies on the verge of 20%. *Presented at the European Materials Research Society 2022 Spring Meeting* (May 31, 2022) K.6.1.
5. Kato, T. et al. Enhanced efficiency of Cd-free Cu(In,Ga)(Se,S)2 minimodule via (Zn,Mg)O second buffer layer and alkali metal post-treatment. *IEEE J. Photovolt.* **7**, 1773–1780 (2017).
6. MiaSolé website. MiaSolé breaks world record again: Large area flexible photovoltaic module with 18.64% efficiency. https://miasole.com/miasole-breaks-world-record-again-large-area-flexible-photovoltaic-module-with-18-64-efficiency/ (2019).
7. Ishizuka, S. et al. Physical and chemical aspects at the interface and in the bulk of CuInSe2-based thin-film photovoltaics. *Phys. Chem. Chem. Phys.* **24**, 1262–1285 (2022).
8. Hedström, J. et al. ZnO/CdS/Cu(In,Ga)Se2 thin film solar cells with improved performance. In *Proc. Conference Record of the 23rd IEEE Photovoltaic Specialists Conference*, Louisville, USA, 1993, pp. 364–371.
9. Contreras, M. A. et al. On the role of Na and modifications to Cu(In,Ga)Se2 absorber materials using thin-MF (M = Na, K, Cs) precursor layers. In *Proc. Conference Record of the 26th IEEE Photovoltaic Specialists Conference*, Anaheim, USA, 1997, pp. 359–362.
10. Rudmann, D. et al. Efficiency enhancement of Cu(In,Ga)Se2 solar cells due to post-deposition Na incorporation. *Appl. Phys. Lett.* **84**, 1129–1131 (2004).
11. Chirilă, A. et al. Potassium-induced surface modification of Cu(In,Ga)Se2 thin films for high-efficiency solar cells. *Nat. Mater.* **12**, 1107–1111 (2013).
12. Jackson, P. et al. Effects of heavy alkali elements in Cu(In,Ga)Se2 solar cells with efficiencies up to 22.6%. *Phys. Status Solidi RRL* **10**, 583–586 (2016).
13. Nakamura, M. et al. Cd-free Cu(In,Ga)(Se,S)2 thin-film solar cell with record efficiency of 23.35%. *IEEE J. Photovolt.* **9**, 1863–1867 (2019).
14. Ishizuka, S., Taguchi, N. & Fons, P. J. Similarities and critical differences in heavy alkali-metal rubidium and cesium effects on chalcopyrite Cu(In,Ga)Se2 thin-film solar cells. *J. Phys. Chem. C.* **123**, 17757–17764 (2019).
15. Ishizuka, S. & Fons, P. J. Lithium-doping effects in Cu(In,Ga)Se2 thin-film and photovoltaic properties. *ACS Appl. Mater. Interfaces* **12**, 25058–25065 (2020).
16. Nishinaga, J. et al. Effects of long-term heat-light soaking on Cu(In,Ga)Se2 solar cells with KF postdeposition treatment. *Appl. Phys. Express* **10**, 092301 (2017).
17. Khatri, I., Matsuura, J., Sugiyama, M. & Nakada, T. Effect of heat-bias soaking on cesium fluoride-treated CIGS thin film solar cells. *Prog. Photovolt. Res. Appl.* **27**, 22–29 (2019).
18. Lundberg, O., Edoff, M. & Stolt, L. The effect of Ga-grading in CIGS thin film solar cells. *Thin Solid Films* **480–481**, 520–525 (2005).
19. Erslev, P. T., Lee, J., Hanket, G. M., Shafarman, W. N. & Cohen, J. D. The electronic structure of Cu(In1-xGax)Se2 alloyed with silver. *Thin Solid Films* **519**, 7296–7299 (2011).
20. Chen, L., Lee, J. & Shafarman, W. N. The comparison of (Ag,Cu)(In,Ga)Se2 and Cu(In,Ga)Se2 thin films deposited by three-stage coevaporation. *IEEE J. Photovolt.* **4**, 447–451 (2014).
21. Yoon, J.-H. et al. Electrical properties of CIGS/Mo junctions as a function of MoSe2 orientation and Na doping. *Prog. Photovolt. Res. Appl.* **22**, 90–96 (2014).
22. Yang, S.-C. et al. Silver-promoted high-performance (Ag,Cu)(In,Ga)Se2 thin-film solar cells grown at very low temperature. *Sol. RRL* **5**, 2100108 (2021).
23. Weiss, T. P., Ehre, F., Serrano-Escalante, V., Wang, T. & Siebentritt, S. Understanding performance limitations of Cu(In,Ga)Se2 solar cells due to metastable defects—a route toward higher efficiencies. *Sol. RRL* **5**, 2100063 (2021).
24. Stanbery, B. J., Abou-ras, D., Yamada, A. & Mansfield, L. CIGS photovoltaics: reviewing an evolving paradigm. *J. Phys. D: Appl. Phys.* **55**, 173001 (2022).
25. Nishinaga, J., Kamikawa, Y., Koida, T., Shibata, H. & Niki, S. Degradation mechanism of Cu(In,Ga)Se2 solar cells induced by exposure to air. *Jpn. J. Appl. Phys.* **55**, 072301 (2016).
26. Gecys, P. et al. Scribing of thin-film solar cells with picosecond and femtosecond lasers. *J. Laser Micro Nanoeng.* **7**, 33–37 (2012).

27. Narazaki, A. et al. Evaluation of femtosecond laser-scribed Cu(In,Ga)Se$_2$ solar cells using scanning spreading resistance microscopy. *Appl. Phys. Express* **11**, 032301 (2018).

28. Niki, S. et al. CIGS absorbers and processes. *Prog. Photovolt. Res. Appl.* **18**, 453–466 (2010).

29. Ishizuka, S., Shibata, H., Nishinaga, J., Kamikawa, Y. & Fons, P. J. Effects of RbF postdeposition treatment and heat-light soaking on the metastable acceptor activation of CuInSe$_2$ thin film photovoltaic devices. *Appl. Phys. Lett.* **113**, 063901 (2018).

30. Ishizuka, S., Yamada, A., Fons, P. & Niki, S. Texture and morphology variations in (In,Ga)$_2$Se$_3$ and Cu(In,Ga)Se$_2$ thin films grown with various Se source conditions. *Prog. Photovolt. Res. Appl.* **21**, 544–553 (2013).

31. Virtuani, A., Lotter, E. & Powalla, M. Performance of Cu(In,Ga)Se$_2$ solar cells under low irradiance. *Thin Solid Films* **431-432**, 443–447 (2003).

32. Gabor, A. M. et al. High-efficiency CuIn$_x$Ga$_{1-x}$Se$_2$ solar cells made from (In$_x$Ga$_{1-x}$)$_2$Se$_3$ precursor films. *Appl. Phys. Lett.* **65**, 198–200 (1994).

33. Ishizuka, S., Yamada, A., Fons, P. & Niki, S. Flexible Cu(In,Ga)Se$_2$ solar cells fabricated using alkali-silicate glass thin layers as an alkali source material. *J. Renew. Sustain. Energy* **1**, 013102 (2008).

34. Sites, J. R. & Mauk, P. H. Diode quality factor determination for thin-film solar cells. *Sol. Cells* **27**, 411–417 (1989).

35. Hegedus, S. S. & Shafarman, W. N. Thin-film solar cells: Device measurements and analysis. *Prog. Photovolt. Res. Appl.* **12**, 155–176 (2004).

AUTHOR CONTRIBUTIONS

S.I. conceived the idea and designed the research and experiments. S.I. prepared the CIGS solar cells and minimodules with technical support from coworkers listed in the Acknowledgements section and measured and analyzed the device properties, including the calculation of diode parameters, J–V, EQE, SEM, and EBIC measurements. All authors have contributed to the scientific discussion. S.I. wrote the paper. All authors revised and approved the final version of the manuscript.

COMPETING INTERESTS

The authors declare no competing interests.

ADDITIONAL INFORMATION

Correspondence and requests for materials should be addressed to Shogo Ishizuka.

Reprints and permission information is available at http://www.nature.com/reprints

Publisher's note Springer Nature remains neutral with regard to jurisdictional claims in published maps and institutional affiliations.